TU Delft

Delft University of Technology

Adaptive Neural Network-Based PI (ANN-PI) Control for DC Microgrids in Renewable Hydrogen Production Systems

Khodakaramzadeh, S.; Bauer, P.; Vahedi, H.

DOI
10.1109/IECON58223.2025.11221909

Publication date
2025

Document Version
Final published version

Published in
Proceedings of the IECON 2025 – 51st Annual Conference of the IEEE Industrial Electronics Society

Citation (APA)
Khodakaramzadeh, S., Bauer, P., & Vahedi, H. (2025). Adaptive Neural Network-Based PI (ANN-PI) Control for DC Microgrids in Renewable Hydrogen Production Systems. In *Proceedings of the IECON 2025 – 51st Annual Conference of the IEEE Industrial Electronics Society* (IECON Proceedings (Industrial Electronics Conference)). IEEE. https://doi.org/10.1109/IECON58223.2025.11221909

Important note
To cite this publication, please use the final published version (if applicable).
Please check the document version above.

Copyright
Other than for strictly personal use, it is not permitted to download, forward or distribute the text or part of it, without the consent of the author(s) and/or copyright holder(s), unless the work is under an open content license such as Creative Commons.

Takedown policy
Please contact us and provide details if you believe this document breaches copyrights.
We will remove access to the work immediately and investigate your claim.

This work is downloaded from Delft University of Technology.
For technical reasons the number of authors shown on this cover page is limited to a maximum of 10.

Green Open Access added to TU Delft Institutional Repository
as part of the Taverne amendment.

More information about this copyright law amendment
can be found at https://www.openaccess.nl.

Otherwise as indicated in the copyright section:
the publisher is the copyright holder of this work and the
author uses the Dutch legislation to make this work public.

Adaptive Neural Network-Based PI (ANN-PI) Control for DC Microgrids in Renewable Hydrogen Production Systems

Shadi Khodakaramzadeh, Pavol Bauer, *Senior Member, IEEE*, and Hani Vahedi, *Senior Member, IEEE*

Delft University of Technology, Department of Electrical Sustainable Energy, Delft, Netherlands
S.Khodakaramzadeh-1@tudelft.nl, P.Bauer@tudelft.nl, H.Vahedi@tudelft.nl

IECON 2025 – 51st Annual Conference of the IEEE Industrial Electronics Society | 979-8-3315-9681-1/25/$31.00 ©2025 IEEE | DOI: 10.1109/IECON58223.2025.11221909

***Abstract*—This research presents a neural-adaptive control technique for DC microgrids in renewable hydrogen production systems. The proposed approach tackles voltage stability issues arising from variable solar production and fluctuating electrolyzer loads with an adaptive neural network-based proportional-integral (ANN-PI) controller with online system identification. The control architecture utilizes two concurrent multilayer perceptron (MLP) networks: one for real-time system identification to estimate the Jacobian matrix, and another for adaptive proportional-integral (PI) parameter adjustment. The decentralized architecture removes communication dependencies among converters, hence improving reliability and scalability. Simulation results indicate a better dynamic response with a 50% decrease in settling time, increased voltage stability retaining the DC bus voltage within $\pm 2\%$ of the nominal 400 V, and resilient performance under diverse situations, including load transitions and changes in solar irradiation. The neural-adaptive method effectively facilitates intelligent, model-free regulation for electric-hydrogen DC microgrids.**

***Index Terms*—DC microgrid, renewable hydrogen production, neural networks, adaptive control, system identification**

I. Introduction

The need for effective integration of renewable energy sources, especially in off-grid applications, has grown in parallel with the worldwide shift towards sustainable energy systems. The potential of DC microgrids to solve contemporary energy problems has caused them to suddenly become a hot topic in the world of global energy discussion. Hydrogen generation via water electrolysis in DC microgrids is one renewable energy application that has recently attracted a lot of interest due to its potential as a means of decarbonizing industrial processes and storing energy for the future [1]–[3].

DC microgrids are transforming energy systems by providing efficient, dependable, and sustainable solutions to contemporary power grid concerns [4]. These systems improve performance in vital applications like renewable hydrogen production facilities and streamline energy distribution by directly integrating renewable energy sources and removing the inefficiencies of AC-DC conversion. The DC setup has several built-in benefits over AC systems, such less complexity in control and increased efficiency in the lack of reactive power and frequency regulation [5]. However, challenges arise from intermittent solar input, fluctuating load demands from the electrolyzer, and the complex charging/discharging behavior of the battery. Significant DC bus voltage variances, caused by these oscillations, might undermine system stability and decrease the electrolyzer's operating efficiency.

Different strategies for resolving control issues in DC microgrids are revealed in the literature. Decentralized control systems were first proposed as a solution to this challenge. Nonetheless, decentralized control has difficulties coordinating rapid changes owing to inadequate data about the currents and voltages of other power converters [6]. Conventional PI controllers, however prevalent, often fail to sustain maximum performance under diverse operating situations because of their fixed-gain characteristics [7].

Recent studies investigated advanced control mechanisms for renewable hydrogen generation. The energy conversion efficiency of the Hydrogen Production Unit (HPU) is established, and an adaptive strategy for efficiency is formulated. Energy management techniques are categorized into four types: fuzzy logic control [8], model predictive control [9], metaheuristic optimization algorithms, and stochastic/robust programming [10], [11].

Artificial neural networks have surfaced as a viable alternative for microgrid control. A novel energy management technique is developed in a DC microgrid using a hybrid energy storage system controlled by artificial neural networks [12]. The ANN controller is trained using ADP (approximate dynamic programming) with the LM (Levenberg-Marquardt) algorithm [13], and research indicates that the proposed controller effectively sustains voltage stability in standalone DC microgrids and regulates power distribution among parallel-connected distributed generation units [14].

Despite these developments, there hasn't been a thorough analysis that provides a broad grasp of the current methods and upcoming developments in managing DC microgrids with renewable energy incorporated [15]. Most current neural network-based control methodologies either concentrate on optimizing individual components or need intricate communication networks among dispersed controllers, hence limiting their practical application and system dependability [16], [17].

In order to address these issues, this research suggests a closed-loop control architecture that uses an ANN-PI con-

Authorized licensed use limited to: TU Delft Library. Downloaded on November 21,2025 at 10:29:56 UTC from IEEE Xplore. Restrictions apply.

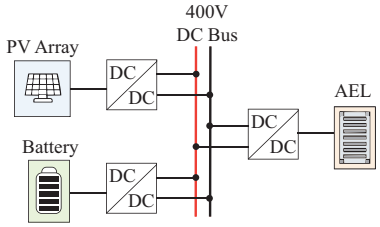

Fig. 1. Typical structure of the renewable hydrogen production system.

troller and a neural-based system identifier. The multi-layer perceptron (MLP)-based system identifier is trained online to provide real-time estimates of the controlled system's Jacobian. With this estimate, the PI controller may adjust the integral and proportional gains according to the error signals and current operating situation. To improve its gains through gradient-based backpropagation, the controller takes three real-time inputs: voltage error and integral of the error and utilizes them. The proposed architecture uses two parallel neural networks: one is used to detect the dynamic behavior of the system, and the other to adjust the PI gains adaptively. Without the need for an explicit system model, the system can dynamically adjust to fluctuations in generation and load due to its dual-network architecture. Reliability and scalability are both improved by eliminating communication lines made possible by the control system's decentralized design. The key contributions of this study are as follows:

- Enhanced Dynamic Response: The ANN-PI controller significantly reduces overshoot and shortens settling time by 50%, ensuring smoother DC bus regulation.
- Improved Voltage Stability: It minimizes voltage ripple, ensuring cleaner and more stable DC output under steady-state conditions.
- Robustness to Uncertainties: The system maintains stable operation under nonlinear conditions and rapid disturbances without the need for manual gain tuning.
- Communication-Free Implementation: The decentralized structure needs no centralized control or communication links, enhancing system scalability and reliability.

The simulation results confirm that the proposed controller maintains the DC bus voltage within a $\pm 2\%$ range. These results show that neural-adaptive control supports future electric-hydrogen DC microgrids by enabling intelligent, model-free, scalable control strategies

II. SYSTEM STRUCTURE OF THE ELECTRIC-HYDROGEN MICROGRID

Off-grid DC microgrids are increasingly deployed to support clean energy applications such as hydrogen production via water electrolysis. The configuration of the considered hydrogen DC microgrid is shown in Fig.1. This system, which consists of an alkaline water electrolyzer, a bidirectional battery storage unit, and a photovoltaic (PV) array, is being investigated in off-grid mode. Using suitable power electronic converters, these parts are connected to a common DC bus.

The system is designed to provide rapid energy exchange and voltage stability with minimal conversion steps. The BESS

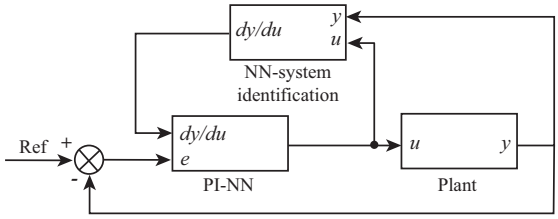

Fig. 2. General block diagram of the proposed control stategy.

acts as a power buffer that either absorbs surplus PV energy or supplies power when generation is insufficient. Due to fluctuating stored energy and renewable input, the electrolyzer imposes a dynamic load. These interactions require precise coordination to ensure reliable system performance, especially without external grid support.

The control flexibility and simplicity design of this configuration are its defining features. Various operational situations need responses from the control system that span various durations. Thus, a real-time adaptive control strategy that can handle both internal and external disturbances is required.

A detailed explanation of the proposed control methodology is provided in the next section.

III. PROPOSED CONTROL STRATEGY OF ELECTRIC-HYDROGEN DC MICROGRID

The general control scheme is structured as depicted in the block diagram in Fig.2. In this setup, two neural networks are used: (1) a neural network for system identification, and (2) a neural network for tuning the parameters of the PI controller. In the proposed methodology, the system is first identified online by the system identification network, which is then used to estimate the system's Jacobian matrix. The PI controller parameters are then calculated adaptively using this Jacobian. The controller gains are optimized based on the error signal. In other words, to minimize the error between the reference and the actual output, and to ensure that the system response closely tracks the desired behavior, the PI parameters are updated adaptively using a gradient descent optimization technique. In the following subsections, each component of the control scheme is explained in detail.

A. Multilayer Perceptron (MLP) Neural Networks

The multilayer perceptron (MLP) based on artificial neural networks (ANNs) is closely inspired by the biological neural computing systems implemented in the human brain. An MLP consists of the inputs, weights, a bias, an activation function, and the output. Initially, models are generated randomly with weight and bias. The neuron takes the weighted sum of the inputs, adds the bias and then applies an activation function for the output. In the training step, the weights are updated gradually in an optimization algorithm to minimize the difference between predicted and actual outputs. Machine learning algorithms have also taken inspiration from how the human brain works and artificial neural networks are the mathematical models used in the simulation of these learning processes.

In MLPs, a supervised learning method called *backpropagation* is commonly used to train the network. The use of multiple layers and nonlinear activation functions distinguishes

Authorized licensed use limited to: TU Delft Library. Downloaded on November 21,2025 at 10:29:56 UTC from IEEE Xplore. Restrictions apply.

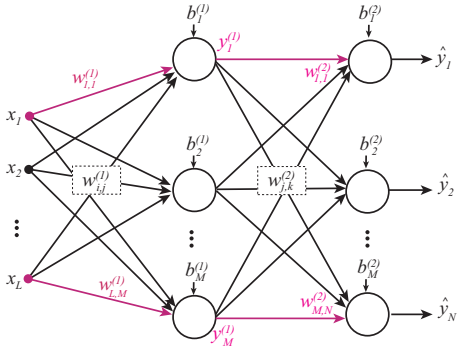

Fig. 3. Two-layer Multi-Layer Perceptron (MLP) neural network.

MLPs from linear perceptrons and enables them to classify nonlinearly separable data.

Fig. 3 illustrates a two-layer MLP neural network. The input layer consists of L inputs $(x_1, x_2, \ldots, x_L)$, which are connected to M neurons in the hidden layer. These connections between the input and the hidden layers are manifested as the weights $w_{i,j}^{(1)}$ and biases $b_j^{(1)}$, where $i = 1, \ldots, L$ and $j = 1, \ldots, M$. The hidden layer outputs are connected to the output layer with weights $w_{j,k}^{(2)}$ and biases $b_k^{(2)}$, where $k = 1, \ldots, N$. Here, N denotes the number of output neurons. The final outputs $\hat{y}_k$ represent the network's predictions. This structure allows the MLP to approximate complex nonlinear mappings between inputs and outputs.

B. ANN-PI Controller Using Gradient Descent Optimization

In this method, a PI controller's parameters are adaptively adjusted using a neural network. As illustrated in Fig. 3, a two-output multi-layer perceptron (MLP) neural network is constructed, corresponding to K_P and K_I, which represent the proportional and integral gains of the PI controller, respectively. The input layer receives two signals: (1) the error signal $x_1 = e(t)$ between the reference value and the measured value, and (2) it's integral value $x_2 = \int e(t)dt$. These inputs are fed into a hidden layer that contains $M = 10$ neurons, a number chosen based on experimental results. The neurons in the hidden layer use the sigmoid activation function, while the output layer uses a linear (identity) activation function as follows:

$$\begin{cases} f_1(x) = \dfrac{1}{1+e^{-x}} \\ f_2(x) = x \end{cases} \tag{1}$$

Here the output layer preserves linearity while the hidden layer uses a sigmoid function (f_1), which squashes inputs into the range $[0, 1]$. For the first lyer, the weight matrix is denoted as $[W]_{i\times j}$, where i is the number of inputs and j is the number of neurons in the hidden layer. The weight matrix for the output layer is $[W]_{j\times k}$, where k represents the number of outputs. The weighted input to the hidden layer neurons, net_1, is computed as the dot product of the input vector x_i and the first-layer weight matrix $W_{i,j}$:

$$net_1 = x_i \times [W]_{i\times j} \tag{2}$$

The first layer's activation function processes the weighted input net_1, producing the output $o_1 = f_1(net_1)$:

$$o_1 = \frac{1}{1+e^{-net_1}} \tag{3}$$

The second layer's input, net_2, is similarly determined by $net_2 = o_1 \cdot [W]_{j\times k}$. Finally, net_2 is passed through its activation function $o_2 = f_2(net_2) = net_2$ to obtain the output of the second layer (output layer).

It should be pointed out that each of the PI controller parameters (K_p and K_i) can also be obtained separately based on parallel neural networks with two inputs and one output. However, this method increases the computational burden and estimation time. Each approach, nevertheless, can be applied in different systems to choose the most suitable closed-loop configuration depending on the desired performance.

A key technique in deep learning for artificial neural networks with multiple hidden layers is backpropagation. It is employed to more precisely calculate the weights' gradient, allowing for the stabilization of the neuron weights and effective learning algorithm optimization. Feedforward neural networks trained with supervised learning frequently use this algorithm. This strategy aims to optimize a cost function. The cost function in this method is defined as:

$$Q_1(k) = \frac{1}{2}e^2(k) = \frac{1}{2}\left(d(k) - y(k)\right)^2 \tag{4}$$

where $d(k)$ is the target value and $y(k)$ is the output generated by the perceptron. This method provides the following update rule for the first and second layer weights:

$$w_i(k+1) = w_i(k) - \eta\frac{\partial Q_1(k)}{\partial w_i(k)} \quad \text{for } i = 1, 2 \tag{5}$$

where η is the learning rate, and $w_i(k)$ are the weight matrices of the first and second layers, respectively. Futhermore, the gradient with regard to the weights of the second (output) layer is computed as:

$$\frac{\partial Q_1(k)}{\partial w_2(k)} = \frac{\partial Q_1(k)}{\partial e(k)} \cdot \frac{\partial e(k)}{\partial y(k)} \cdot \frac{\partial y(k)}{\partial o_2(k)} \cdot \frac{\partial o_2(k)}{\partial \text{net}_2(k)} \cdot \frac{\partial \text{net}_2(k)}{\partial w_2(k)} \tag{6}$$

$$\frac{\partial Q_1(k)}{\partial w_2(k)} = -e(k) \cdot \frac{\partial y(k)}{\partial o_2(k)} \cdot F_2' \cdot o_1 \tag{7}$$

Similarly, the gradient with respect to hidden layer weights is:

$$\frac{\partial Q_1(k)}{\partial w_1(k)} = -e(k) \cdot \frac{\partial y(k)}{\partial o_2(k)} \cdot F_2' \cdot w_2 \cdot F_1' \cdot x_i \tag{8}$$

The gradient expressions derived above are used to update the neural network weights using the gradient descent algorithm. One limitation of such methods, however, is that the system output derivative with respect to the neural network output (the system Jacobian) is required. Using model-free methods has limitations as it still needs a system model.

C. Neural Identifier for Controlled Systems

Neural networks are powerful tools for identifying nonlinear systems. The block diagram of the proposed closed-loop control system is shown in Fig. 4. In this setup, the controlled system is estimated using a neural identifier, and the error between the plant output y_p and the identifier output y_m is

Authorized licensed use limited to: TU Delft Library. Downloaded on November 21,2025 at 10:29:56 UTC from IEEE Xplore. Restrictions apply.

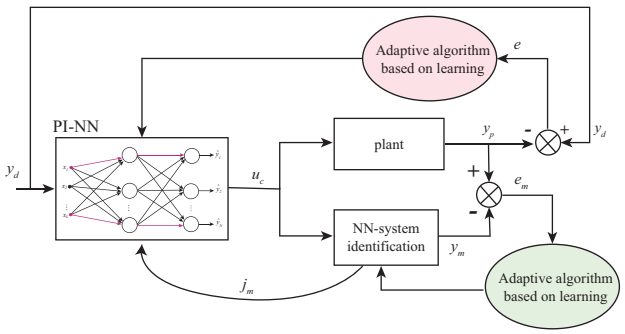

Fig. 4. Block diagram of the proposed control stategy with more details.

minimized by adapting the identifier's parameters via a learning algorithm. The system's Jacobian J_m is then estimated and used by an adaptive neural PI controller to compute the control signal u_c at each sampling time. A Multilayer Perceptron (MLP) is employed as the neural identifier. The plant's Jacobian is approximated as:

$$\frac{\partial y_p(k)}{\partial u_c(k)} \approx \frac{\partial y_m(k)}{\partial u_c(k)}; \quad J_p(k) \approx J_m(k), \tag{9}$$

where $y_p(k)$ is the plant output, $u_c(k)$ is the control signal, and $y_m(k)$ is the neural identifier's output. The identifier's input is u_c, and its weights are updated using gradient descent.

- **Layer 1**: Input u_c is multiplied by weights $[\vartheta_1]_{1\times m}$, producing net_1, which is then passed through an activation function F_1 to output o_1.
- **Layer 2**: o_1 is multiplied by the weights $[\vartheta_1]_{m\times 1}$, which gives net_2. Then, the final output $o_2 = y_m$ is obtained.

The cost function is defined as:

$$Q_2(k) = \frac{1}{2}e_m^2(k) = \frac{1}{2}\left(y_p(k) - o_2(k)\right)^2. \tag{10}$$

To minimize $Q_2(k)$, gradient descent updates the weights:

$$\vartheta_i(k+1) = \vartheta_i(k) - \gamma\frac{\partial Q_2(k)}{\partial \vartheta_i(k)}, \tag{11}$$

where γ is the learning rate. The weight updates for both layers of the neural identifier are derived through backpropagation. For the output layer weights ϑ_2, the gradient of the cost function $Q_2(k)$ is obtained as:

$$\frac{\partial Q_2(k)}{\partial \vartheta_2(k)} = -e_m(k)F_2'(\text{net}_2(k))o_1(k) \tag{12}$$

where F_2' is the derivative of the output layer activation function. For the hidden layer weights ϑ_1, the gradient propagates backward through the network:

$$\frac{\partial Q_2(k)}{\partial \vartheta_1(k)} = -e_m(k)F_2'(\text{net}_2(k))\vartheta_2(k)F_1'(\text{net}_1(k))u_c(k) \tag{13}$$

with F_1' representing the hidden layer activation derivative. These gradients drive the weight adaptation process through gradient descent:

$$\vartheta_i(k+1) = \vartheta_i(k) - \gamma\frac{\partial Q_2(k)}{\partial \vartheta_i(k)} \tag{14}$$

where γ is the learning rate. The derivation follows standard backpropagation principles, with Jacobian of the activation functions ensuring proper error propagation through the network layers. Moreover, the system Jacobian is derived as:

$$J_m(k) = \frac{\partial o_2(k)}{\partial u_c(k)} = F_2'\vartheta_2 F_1'\vartheta_1. \tag{15}$$

This adaptive method continuously modifies the neural identifier and controller settings to ensure proper control.

IV. System Design and Simulation Results

A. System Parameter Design

Fig. 5 shows a schematic of a renewable hydrogen production system that incorporates the suggested control structure. Using a cascaded control technique, the control architecture employs outer voltage loops to produce references for inner current loops. To deal with converter nonlinearities, neural networks are used for both system identification and adaptive control. In particular, the PV converter uses an MPPT controller to maximize energy collection, which has been investigated in many past works. The bidirectional control feature of the battery converter allows it to manage charging and discharging activities as well as regulate the DC bus voltage. To keep the electrolyzer voltage and current under control and the hydrogen production steady, the alkaline electrolyzer (AEL) buck converter is used.

Table I lists the key parameters used in the implementation. A common figure for DC microgrids, 400V was chosen for the DC bus voltage. The power needs of the system dictated the rated currents of the AEL and the battery. The learning rates (η_{kp}, η_{ki}, and γ) for the neural network controllers were optimized via simulation to achieve a compromise between stability and adaptability speed.

The ANN-PI controllers were implemented with focus on the specific requirements of each converter:

- For the PV converter, optimal energy gathering and steady operation were the primary goals.
- For the battery converter, we prioritized excellent DC bus voltage control and SOC management.
- Accurate current management was critical for the AEL converter to produce hydrogen efficiently.

B. Simulation Results

In order to assess the suggested control strategy's efficacy, a detailed simulation scenario was created to reflects realistic operating conditions in renewable hydrogen production systems. The simulation includes multiple operational transitions to test the controller's robustness:

- **Initial Operation (0-2s)**: The electrolyzer operates at its nominal power, simulating the typical circumstances for producing hydrogen.
- **Reduced Load (2-4s)**: The electrolyzer load is reduced to 50% of nominal power to mimic a decrease in hydrogen production caused by demand or energy management.
- **Overload Operation (4-6s)**: To ensure the system can manage transient overload circumstances that may arise during times of high hydrogen demand, the power of the electrolyzer is raised to 110% of its nominal value.

Authorized licensed use limited to: TU Delft Library. Downloaded on November 21,2025 at 10:29:56 UTC from IEEE Xplore. Restrictions apply.

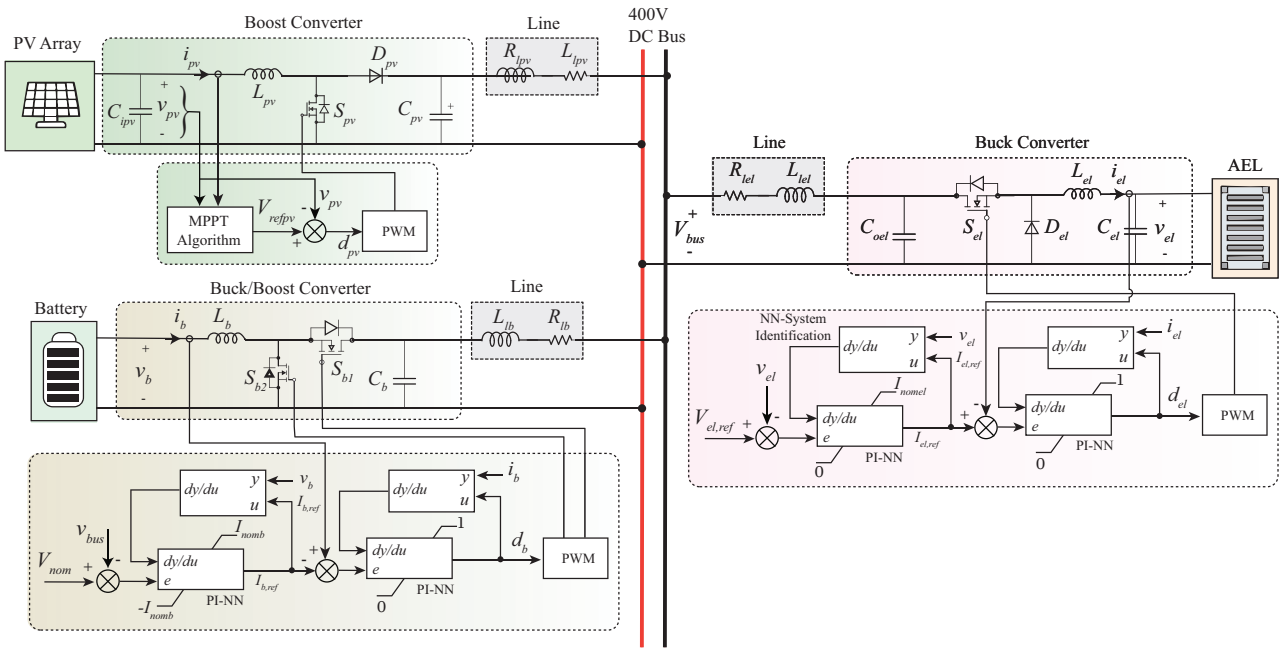

Fig. 5. Typical renewable hydrogen production system with the proposed control structure

TABLE I
SYSTEM PARAMETERS

Parameter	Description	Value
V_{nom}	Nominal DC bus voltage	400 V
I_{nomel}	Rated AEL current	14 A
I_{nomb}	Rated battery current	44 A
Power Converter Parameters		
C_{ipv}	Input capacitance of PV converter	10 μF
L_{pv}	Boost inductor	10 mH
C_{pv}	Output capacitance of PV converter	10 μF
L_b	Buck/boost inductor	0.5 mH
C_b	Output capacitance of battery converter	1 mF
C_{oel}	Input capacitance of AEL converter	220 μF
L_{el}	Buck inductor	1 mH
C_{el}	Output capacitance of AEL converter	470 μF
Line Impedances		
R_{lpv}, R_{lb}, R_{lel}	Line resistances	0.1 Ω
L_{lpv}, L_{lb}, L_{lel}	Line inductances	10 mH
API-NN Control Parameters		
η_{kp}	Proportional term learning rate	0.001
η_{ki}	Integral term learning rate	0.01
γ	Neural network learning rate for identifier	0.001
m	Hidden layer neurons	10 μH
Neural Network Parameters		
$f_1(x)$	Hidden layer activation function	Sigmoid
$f_2(x)$	Output layer activation function	Linear

- **Solar Irradiance Variation (6-8s)**: In this time, solar irradiance drops to half its original value but the overload condition is maintained, leading to a difficult situation where generation drops but load stays high.
- **Solar Irradiance Recovery (8-10s)**: The system's reaction to variations in positive generation may be evaluated after solar irradiance recovers to its former level.

This operational scenario is highly realistic for renewable hydrogen systems, as modern electrolyzers operate across variable power ranges to accommodate the fluctuations in renewable energy sources. Fig. 6 shows the overall system performance under the suggested ANN-PI control technique. During all operational transitions, the proposed ANN-PI controller (solid pink lines) considerably outperforms the conventional PI controller (dashed blue lines) in terms of settling time and overshoot reduction. The conventional PI controller parameters follow the design in in [**?**]. The inset zoomed in shows rapid voltage recovery within 0.1 seconds, and the DC bus voltage regulation (a) maintains excellent stability at 400V nominal with minimal deviations. By comparing the electrolyzer power consumption during nominal power (3kW), reduced load (1.6kW), and overload conditions (4kW), the ANN-PI approach shows better control capability, while the conventional controller shows significant oscillations and poor tracking performance, which could reduce electrolyzer efficiency. During the operating phases, both controllers display identical discharge patterns, demonstrating that the enhanced electrolyzer control does not negatively impact the performance of the energy storage system. This indicates that the battery SOC management (c) effectively coordinates the energy. Under different renewable generation and load situations, the findings show that the neural-adaptive method offers strong system-wide management, guaranteeing stable DC microgrid operation and dependable hydrogen production. Furthermore, Fig. 7 depicts the adaptive evolution of PI gains for both voltage and current control loops, where $k_{p,el}$ and $k_{i,el}$ represent the proportional and integral gains for the electrolyzer converter, while $k_{p,b}$ and $k_{i,b}$ correspond to the proportional and integral gains for the battery converter. At $t = 2s$, $t = 4s$, and $t = 8s$, which correspond to load transitions, the neural networks make significant modifications

Authorized licensed use limited to: TU Delft Library. Downloaded on November 21,2025 at 10:29:56 UTC from IEEE Xplore. Restrictions apply.

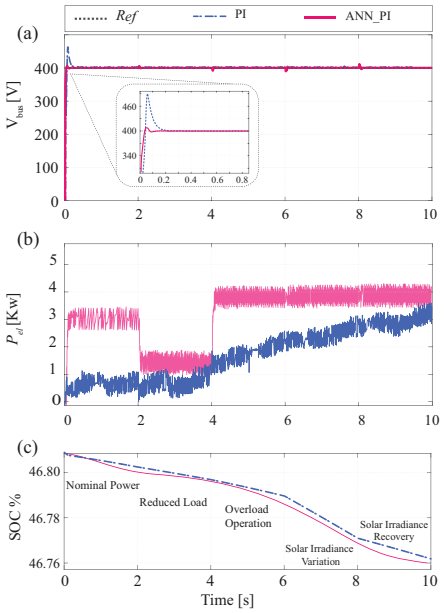

Fig. 6. Comparative system performance: (a) DC bus voltage regulation, (b) electrolyzer power consumption, (c) battery SOC management under ANN-PI vs conventional PI control.

to these parameters in reaction to changing conditions. To maintain system stability under varying operating circumstances, the gains quickly converge to new optimum levels after each transition. This parameter adaptation demonstrates the effectiveness of the neural-adaptive approach in eliminating the need for manual tuning while maintaining optimal performance throughout varied operational scenarios.

The results demonstrate that the neural-adaptive control approach successfully tackles the obstacles in renewable hydrogen production systems, offering consistent performance under various operating conditions.

In our future work, we will focus on formulating advanced energy management solutions for this sustainable hydrogen microgrid.

V. Conclusion

This paper provides a neural-adaptive control technique for DC microgrids in renewable hydrogen production systems. The proposed ANN-PI controller with online system identification effectively eliminates the voltage stability issues arising from variable solar production and oscillating electrolyzer loads. Main results include a 50% decrease in settling time, $\pm 2\%$ accurate in voltage regulation, and reliable performance without the need of manual adjustment. The decentralized design removes communication dependencies, hence improving reliability and scalability. The simulation results confirm the controller's effectiveness.

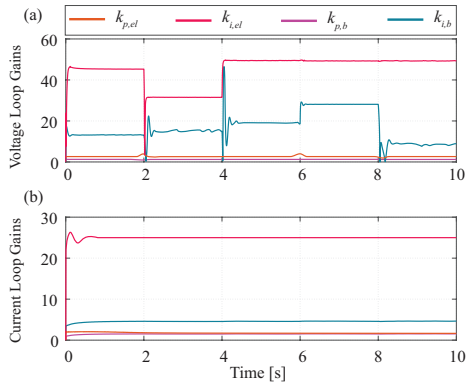

Fig. 7. Adaptive evolution of PI controller gains: (a) voltage loop controller gains and (b) current loop controller gains

References

[1] S. A. Bonab, T. Waite, W. Song, D. Flynn, and M. Yazdani-Asrami, "Machine learning-powered performance monitoring of proton exchange membrane water electrolyzers for enhancing green hydrogen production as a sustainable fuel for aviation industry," *Energy Reports*, vol. 12, pp. 2270–2282, 2024.

[2] H. Armghan, Y. Xu, H. Sun, N. Ali, and J. Liu, "Event-triggered multi-time scale control and low carbon operation for electric-hydrogen dc microgrid," *Applied Energy*, vol. 355, p. 122149, 2024.

[3] R. S. Deshmukh, G. Rituraj, N. Lock, H. Vahedi, A. Shekhar, and P. Bauer, "Implementation of real-time digital twin of dual active bridge converter in electrolyzer applications," in *IECON 2023-49th Annual Conference of the IEEE Industrial Electronics Society*. IEEE, 2023, pp. 1–6.

[4] H. Vahedi and M. Trabelsi, *Single-DC-Source Multilevel Inverters*. Springer, 2019.

[5] H. Vahedi, "5-level packed u-cell (puc5) active front-end rectifier," *IEEE Open Journal of Power Electronics*, vol. 6, pp. 1022–1027, 2025.

[6] M. Trabelsi, H. Vahedi, and H. Abu-Rub, "Review on single-dc-source multilevel inverters: Topologies, challenges, industrial applications, and recommendations," *IEEE Open Journal of the Industrial Electronics Society*, vol. 2, pp. 112–127, 2021.

[7] M. Trabelsi, A. N. Alquennah, and H. Vahedi, "Review on single-dc-source multilevel inverters: Voltage balancing and control techniques," *IEEE Open Journal of the Industrial Electronics Society*, vol. 3, pp. 711–732, 2022.

[8] R. Rodriguez, J. P. F. Trovão, and J. Solano, "Fuzzy logic-model predictive control energy management strategy for a dual-mode locomotive," *Energy Conversion and Management*, vol. 253, p. 115111, 2022.

[9] M. B. Abdelghany, V. Mariani, D. Liuzza, and L. Glielmo, "Hierarchical model predictive control for islanded and grid-connected microgrids with wind generation and hydrogen energy storage systems," *International Journal of Hydrogen Energy*, vol. 51, pp. 595–610, 2024.

[10] L. P. Van, K. Do Chi, and T. N. Duc, "Review of hydrogen technologies based microgrid: Energy management systems, challenges and future recommendations," *International Journal of Hydrogen Energy*, vol. 48, no. 38, pp. 14 127–14 148, 2023.

[11] Q. Shafiee, J. M. Guerrero, and J. C. Vasquez, "Distributed secondary control for islanded microgrids—a novel approach," *IEEE Transactions on power electronics*, vol. 29, no. 2, pp. 1018–1031, 2013.

[12] H. Vahedi, P.-A. Labbé, and K. Al-Haddad, "Sensor-less five-level packed u-cell (puc5) inverter operating in stand-alone and grid-connected modes," *IEEE Transactions on Industrial Informatics*, vol. 12, no. 1, pp. 361–370, Feb 2016.

[13] H. Vahedi and K. Al-Haddad, "Method and system for operating a multilevel electric power inverter," US Patent, 2018, uS9923484B2.

[14] W. Dong, S. Li, and X. Fu, "Artificial neural network control of a standalone dc microgrid," in *2018 Clemson university power systems conference (PSC)*. IEEE, 2018, pp. 1–5.

[15] M. S. Alam, M. A. Hossain, M. Shafiullah, A. Islam, M. Choudhury, M. O. Faruque, and M. A. Abido, "Renewable energy integration with dc microgrids: Challenges and opportunities," *Electric Power Systems Research*, vol. 234, p. 110548, 2024.

[16] R. S. Deshmukh, G. Rituraj, P. Bauer, and H. Vahedi, "Real-time digital twin implementation of power electronics-based hydrogen production system," *Energy Reports*, vol. 13, pp. 5006–5015, 2025.

[17] H. Bevrani, F. Habibi, P. Babahajyani, M. Watanabe, and Y. Mitani, "Intelligent frequency control in an ac microgrid: Online pso-based fuzzy tuning approach," *IEEE transactions on smart grid*, vol. 3, no. 4, pp. 1935–1944, 2012.

Authorized licensed use limited to: TU Delft Library. Downloaded on November 21,2025 at 10:29:56 UTC from IEEE Xplore. Restrictions apply.